Numerical simulation of H_2S and CO_2 generation during SAGD

A. PEREZ-PEREZ, A.M. KAMP
CHLOE, UFR Science, University of Pau, 64000, Pau, France

H. SOLEIMANI
IFP School, 1-4 avenue de Bois Preau, 92500 Rueil-Malmaison, France

G. DARCHE
TOTAL, CSTJF, 64000, Pau, France (now with TOTAL EP Congo)

Abstract

The production of undesirable gases during thermal projects such as Steam-Assisted Gravity Drainage (SAGD) applied to heavy oils has been widely observed. The increase in temperature and the presence of water promote chemical reactions that generate the production of hydrogen sulphide and carbon dioxide and in minor amounts some other gases. This process is called aquathermolysis. Studies of this gas generation process have been reported in literature, but its prediction has not been integrated in reservoir simulation.

The objective of our work is to develop, using experimental data from literature, a kinetic model for H_2S and CO_2 generation by aquathermolysis, and to integrate this model in reservoir simulation.

We consider H_2S being formed from organosulphuric oil compounds and CO_2 from an inorganic source. Kinetic models for the creation of both types of components are based on sets of multiple parallel reactions leading to production plateaus that are a function of temperature. Partition coefficients are then introduced for H_2S and CO_2 as a function of temperature and pressure allowing these components to appear in gas, oil and water phases.

We show predictions of H_2S, CO_2 and solution gas production under conditions typically found in Athabasca oil sands during SAGD operations. Simulation results appear to be very sensitive to the kinetics of H_2S and CO_2 generation. Matching and prediction of gas production levels requires therefore reliable experimental data for this kinetics. Simulation results can be analysed to better understand aquathermolysis mechanisms in the reservoir (location of reactions and transport of H_2S and CO_2 in fluid phases).

Introduction

The injection of steam during thermal recovery of bitumen implies chemical reactions between some heavy oil components, sand and water. The term aquathermolysis originally proposed by Hyne (1982) was used to describe these chemical reactions during steam injection of heavy oils. In general, significant amounts of hydrogen sulphide and carbon dioxide are generated while minor quantities of hydrogen and light oil components have been detected in thermal recovery projects such as Steam Assisted Gravity Drainage (SAGD). Values of hydrogen sulphide produced per ton of bitumen during aquathermolysis has been reported to vary between 6 and 75 liters at standard conditions (Thimm 2000, 2008) while concentration in the range of 30 and 20.000 ppm in produced gas has been observed at steam injection conditions (T≤240°C) in Venezuela (Hyne, 1986). Experimental studies have shown that the generation of CO_2 is always higher and sometimes even much higher than that of H_2S. Usually it is in the range 900-10,000 liters per tonne at standard conditions, being generally the major component of the gas phase produced during aquathermolysis.

Laboratory tests performed by Hyne (1982, 1986) consisted in studying the reaction between Canadian and Venezuelan heavy oil sands and saturated water in a range of temperature between 200 and 300°C. They employed a vessel made of a

material with a high content of cobalt and nickel which may have catalyzed chemical reactions. According to his results, the gas production was catalyzed by the reactor walls but the final equilibrium value at 90 days was the same as that reached in an uncatalyzed system (quartz tube) over a longer period of time.

For both studied oil sands, an upper limit of gas production was detected at different temperatures, indicating a relationship between the gas production capacity and temperature. The formation of this plateau indicates the presence of labile reactive components that vary (increase) with temperature exposition. This behaviour was found for both CO_2 and H_2S gas production by Hyne (1982, 1986) and Clark et al (1985).

Lamoureux and Lorant (2005a) studied the H_2S formation in Athabasca oil sands submitted to steam injection. They measured the amount of H_2S generated during aquathermolysis in the typical range of temperature found in the steam chamber. Similar to Hyne results, a maximum of H_2S gas production was observed at different times and temperatures, indicating the existence of a limited content of reactive components. In addition, the authors studied the H_2S source. They verified the hypothesis proposed by Hyne (1982, 1984) that suggested that a correlation exists between the amount of H_2S generated and its content in organic sulphur compounds. They found that small fractions of these are labile, in general, lower than 1 % wt. of the total organic sulphur in oil sands (Lamoureux & Lorant, 2005b).

The source of CO_2 from heavy oil sands submitted to a thermal process has been well documented in literature. Hyne (1982, 1984) thought that much of the CO_2 produced may have come from decarboxylation of carboxylic acid adsorbed on sand grains. However, he also found that significant quantities of carbon dioxide are produced during the aquathermolysis of sand from which oil was extracted. Abercrombie and Hutcheon (1986) and Cathles et al (1987, 1990) have shown evidences for CO_2 coming mostly from carbonate decomposition during steamflooding. Through measurement of carbon isotopes in produced fluid, they were able to show that the evolved CO_2 was mainly inorganic in origin. Gunter and Bird (1988) found that relatively clean quartz from Cold Lake can generate CO_2 production under steam injection conditions. CO_2 production has been reported for different sands having a different mineralogy (Abercrombie and Hutcheon, 1986; Cathles et al, 1987). Important CO_2 quantities have been detected even at temperature as low as 200°C (Bird et $al.$, 1986).

Concerning the modeling of H_2S and CO_2 generation under steam injection using a reservoir simulator, not much work has been published (Salazar et al, 1989, Gillis and Thimm, 2000). In particular, Gillis and Thimm did some forecasts of gas production in SAGD using a model based on gas dissolution. They did as if the carbon dioxide is sourced in the water phase while the hydrogen sulphide is present in the oil phase and the reaction time is negligible compared to the field time scale. Equilibrium values were calculated based on Henry constants. No chemical reactions were described. CO_2 solubility in oil phase was not specified.

The objective of our work is to quantify gas production for Athabasca bitumen submitted to a SAGD process. This will be done through a conceptual numerical model using a reservoir simulation (STARS from CMG). For predicting gas production, a set of parallel reactions which follows a decomposition kinetics that varies with temperature is described for H_2S and CO_2. This implies that, if temperature is increased, more reactions "become active" allowing a production plateau to be reached faster. Furthermore, thermodynamic equilibrium is described for the generated gases which allow produced gases partition in three phases. In conclusion, a complete model of gas production is proposed and tested at steam injection conditions for a SAGD system.

The authors hope that the proposed model permits estimation of H_2S and CO_2 production in heavy oil reservoirs submitted to steam injection. Results from this model can be used in the design of treatment facilities that allow reduction of environmental damage and prevention of safety problems during the reservoir exploitation period.

Experimental data

Gas production data were taken from results reported in literature. Equilibrium values considered in this work were reported by Hyne (1982, 1986) for the H_2S and by Hyne & Tyrer (1984), Hyne & Clark (1985) and Clark et al (1988) for the CO_2. Table 1 summarizes the equilibrium yields of the H_2S and CO_2 from laboratory aquathermolysis of Athabasca bitumen between 180° and 240°C after 90 days of reaction time. Equilibrium values were obtained by extending plots of gas production versus reaction time to the equilibrium time reported for the experiments (90 days). Other temperatures and times not reported in literature, were obtained by linear data interpolation.

A characterisation of an Athabasca oil sand is detailed in Table 2. An elemental analysis of resin and asphaltene fractions is also described. Both fractions are supposed to be the source of H_2S in the model described below.

Model description

H_2S source

It was assumed that H_2S evolves from some organosulphur compounds contained in resins and asphaltenes. This observation is supported by Lamoureux & Lorant (2005a,b) experiments in which they studied the evolution of sulphur distribution over SARA fractions of Athabasca oil sand at different steam injection temperatures. They concluded that during aquathermolysis sulphur in asphaltenes and in resins is the major source of H_2S found in gas phase. In our model the reactive sulphur specie (HCS_r) is defined as a mixture of reactive fractions of asphaltenes and resins in bitumen. For estimating the initial molar quantity of HCS_r the following assumptions were made:

1) H_2S production results from sulphur liberation of asphaltenes and resins.
2) The reactive sulphur specie (HCS_r) is constituted by the addition of a reactive fraction of resins and a reactive fraction of asphaltenes in oil.
3) Molecular weight and empirical formulas of reactive asphaltenes and reactive resins are equal to molecular weight and empirical formulas of resins and asphaltenes in bitumen. Empirical formulas are derived from elemental analysis.
4) "Reactive resins to reactive asphaltene" molar ratio is equal to resins to asphaltene molar ratio in bitumen.

The initial mole fraction of HCS_r is derived after solving simultaneously assumption (4) and a sulphur mass balance per kg of bitumen. Unknowns are mole fraction of reactive asphaltenes and mole fraction of reactive resins per mole of bitumen. The sulphur mass balance relates the total sulphur in reactive asphaltenes and in reactive resins to the total labile sulphur (produced as H_2S) per kg of bitumen. The total labile sulphur per kg of bitumen is estimated after converting Hyne's equilibrium results (Table 1) into labile sulphur mass fraction of total sulphur available per kg of oil sand. Figure 1 shows this

relation as a function of temperature. According to this figure, the fraction of sulphur that is able to generate H$_2$S during steam injection process is around 0.2 % of the total sulphur contained in bitumen at steam injection temperature of 240°C. The system of two equations is solved at different temperatures (T= 180, 200, 220 and 240°C) where mole fractions of reactive components, HCS$_r$, are calculated. Table 3 shows calculated mole fractions of distributed reactive components.

Furthermore, the total quantity of reactive component can be calculated by the following expression that relates the number of mole of reactive components available for temperature interval i

$$N_{reactive}(i) = \sum_{p} n_{reactive}(p) \quad\text{... (1)}$$

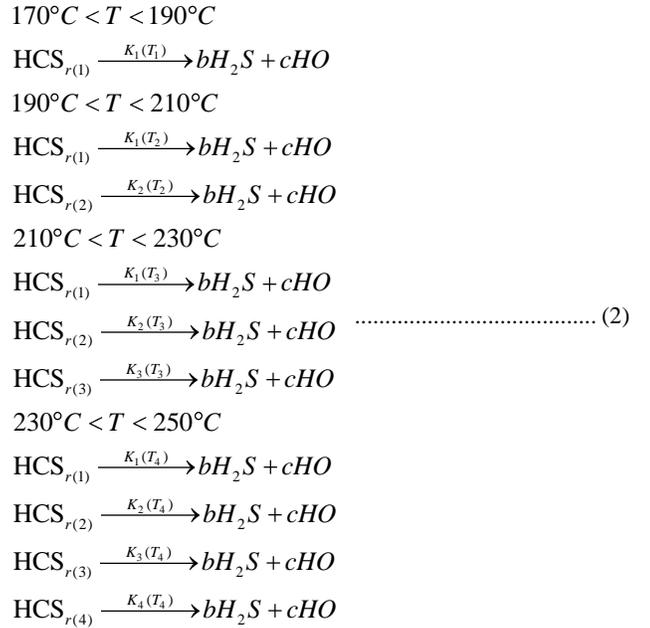with $p \in [1... i]$ and $i \in [1... 4]$.

Kinetic model for H$_2$S generation

The fact that H$_2$S generation is not only a function of equilibrium time but also of temperature suggests that its kinetic model can be represented numerically through a set of parallel reactions. The fact that reactions run in parallel permits the formation of plateaus for different temperatures once the equilibrium time has been reached as was observed by Hyne (1982) and Clark *et al* (1985). This implies that several reactive components exist, and that each one follows particular kinetics.

For describing a kinetic model that takes into account the decomposition of sulphur components, a system with four reactive components, HCS$_r$(1−4) , associated to four temperature intervals, is defined. In this system, each reactive component reaches total conversion at equilibrium time in its corresponding temperature interval: reaction rate is zero below the corresponding temperature interval and reaction rate increases above the corresponding temperature interval.

In the proposed H$_2$S kinetic model, the reactive sulphur component (HCS$_r$) breaks down into H$_2$S in oil phase and original bitumen (HO). H$_2$S can exist also in aqueous and gas phase according to an equilibrium model that will be described later.

The following assumptions were made for the H$_2$S kinetics model:
1. All reactions are first-order decomposition reactions.
2. Temperature intervals start at 170°C and end at 250°C. The temperature interval size is 20°C. Temperature intervals were chosen in a way that temperatures 180, 200, 220 and 240°C were in the middle of the range as these temperatures correspond to those employed to distribute the initial quantity of reactive components.
3. The reaction rate is directly proportional to the rate constant, $K_i(T)$. The constant velocity follows the typical Arrhenius expression composed by a pre-exponential factor and activation energy.
4. Reactions reach full conversion at the end of the equilibrium time (90 days).
5. Reactions have similar stoichiometric coefficients.

The proposed H$_2$S model is described as followed:

$170°C < T < 190°C$

$$HCS_{r(1)} \xrightarrow{K_1(T_1)} bH_2S + cHO$$

$190°C < T < 210°C$

$$HCS_{r(1)} \xrightarrow{K_1(T_2)} bH_2S + cHO$$

$$HCS_{r(2)} \xrightarrow{K_2(T_2)} bH_2S + cHO$$

$210°C < T < 230°C$

$$HCS_{r(1)} \xrightarrow{K_1(T_3)} bH_2S + cHO$$

$$HCS_{r(2)} \xrightarrow{K_2(T_3)} bH_2S + cHO \quad\text{..................................... (2)}$$

$$HCS_{r(3)} \xrightarrow{K_3(T_3)} bH_2S + cHO$$

$230°C < T < 250°C$

$$HCS_{r(1)} \xrightarrow{K_1(T_4)} bH_2S + cHO$$

$$HCS_{r(2)} \xrightarrow{K_2(T_4)} bH_2S + cHO$$

$$HCS_{r(3)} \xrightarrow{K_3(T_4)} bH_2S + cHO$$

$$HCS_{r(4)} \xrightarrow{K_4(T_4)} bH_2S + cHO$$

The stoichiometric coefficients are b=2.15 and c=1.965.

Considering that detailed information about decomposition of this hypothetical reaction system was unknown, a disappearance model of reactive components as a function of time and temperature was proposed. In this model, data from Hyne's experiments (1986) and data from extrapolation of these results at equilibrium time of 90 days (Hyne, 1982; 1986) shown in Table 1 were taking into account. Knowing that the disappearance rate of reactive component follows a first order reaction rate

$$\frac{dn_{reactive}(i)}{dt} = -K_i(T) \cdot n_{reactive}(i) \quad\text{... (3)}$$

The total quantity of reactive component is obtained after integrating the previous expression between 0 and t. The resulting total quantity of reactive component is

$$n_{reactive}(i) = n_{reactive}(i)_{(initial)} \cdot \exp(-K_i(T) \cdot t) \quad\text{.......................... (4)}$$

where

$$K_i(T) = \begin{cases} 0 & , \quad T < T_i \\ A_i \cdot \exp^{-\frac{Ea_i}{RT}} , & T \geq T_i \end{cases} \quad\text{.. (5)}$$

Knowing the initial values for each reactive component from Table 3 and the hypothetical degradation of components as a function of temperature at different times, rate constants can be estimated from equation (4). The fitted kinetic parameters, pre-exponential factor, *A*, and activation energy, *Ea*, are derived from equation (5). Table 4 summarized the kinetic parameters for the H$_2$S generation model.

The total quantity of generated H$_2$S in the whole temperature interval is obtained from the following expression

$$N_{H2S} = b \cdot \sum_i n_{HCS-r}(i)_{initial} \cdot 1 - \exp(-K_i(T_i) \cdot t) \quad \text{.............. (6)}$$

Figure 2 shows the total amount of H_2S generated per kg of oil sand obtained after applying equation (6) and (5), and kinetic parameters from Table 4. The values of H_2S generated at equilibrium time of 90 days (called "reference" in the figure) correspond to the results from Table 1. Hyne's experimental results for two temperatures are also shown. In general, the generated H_2S model reproduce well the experimental observation obtained by Hyne (1982, 1986).

CO$_2$ source

According to literature results produced CO_2 comes from inorganic source. In the model proposed in our work, CO_2 will be generated from rocks. Due to the fact that the reservoir model will not consider the reservoir mineralogy, some pseudo components called reactive sand, $Sand_r$, will be introduced in the model. Four pseudo components will be used to describe the carbon dioxide formation during steam injection. The distributed reactive components will be associated to reacting temperature intervals to permit the formation of plateaus for temperature intervals.

Table 3 shows calculated molar fractions of distributed reactive sand that where obtained from CO_2 results shown in Table 1. The total quantity of reactive sand per temperature interval i can be calculated from equation (1).

Kinetic model for CO$_2$ generation

The fact that CO_2 generation tends to a constant gas production value at specific temperature once the equilibrium time is reached, implies that its kinetic model can be represented numerically through a set of parallel reactions. For describing this kinetic model, a system with four reactive components, $Sand_r$, associated to four temperature intervals is defined. In this system, each reactive component reaches total conversion at equilibrium time in its corresponding temperature intervals: reaction rate is zero below the corresponding temperature interval and reaction rate advances faster above the corresponding temperature interval. This implies that the four reactive components follow a particular kinetics at each temperature interval.

In the proposed CO_2 kinetics model, reactive sand breaks down into CO_2 in water phase. CO_2 exists also in oil and gas phases according to an equilibrium model that will be described later. For simplicity molecular weight of reactive sand was assumed to be equal to molecular weight of carbon dioxide.

For building the CO_2 kinetics model, the assumptions (1) to (5) described for the H_2S model were also employed. The proposed CO_2 model is described as follows:
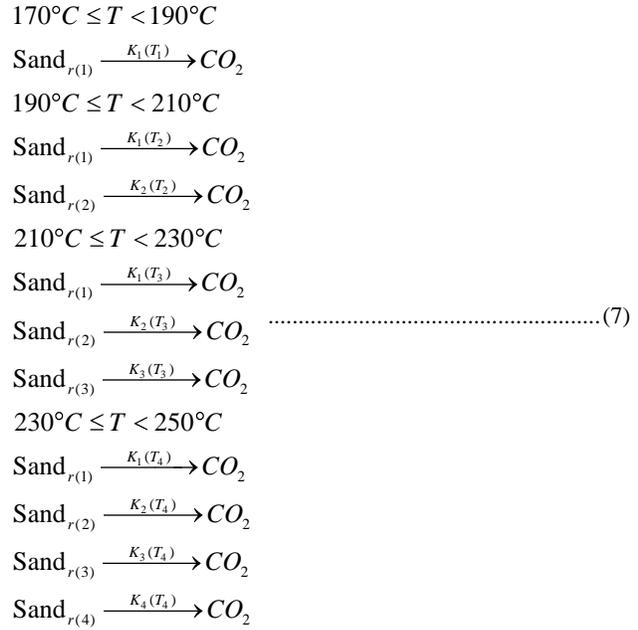
$170°C \leq T < 190°C$

$$Sand_{r(1)} \xrightarrow{K_1(T_1)} CO_2$$

$190°C \leq T < 210°C$

$$Sand_{r(1)} \xrightarrow{K_1(T_2)} CO_2$$

$$Sand_{r(2)} \xrightarrow{K_2(T_2)} CO_2$$

$210°C \leq T < 230°C$

$$Sand_{r(1)} \xrightarrow{K_1(T_3)} CO_2$$

$$Sand_{r(2)} \xrightarrow{K_2(T_3)} CO_2 \quad \text{.....................................(7)}$$

$$Sand_{r(3)} \xrightarrow{K_3(T_3)} CO_2$$

$230°C \leq T < 250°C$

$$Sand_{r(1)} \xrightarrow{K_1(T_4)} CO_2$$

$$Sand_{r(2)} \xrightarrow{K_2(T_4)} CO_2$$

$$Sand_{r(3)} \xrightarrow{K_3(T_4)} CO_2$$

$$Sand_{r(4)} \xrightarrow{K_4(T_4)} CO_2$$

Considering that detailed information about decomposition of this hypothetical reactive system is unknown, a disappearance model of reactive sands as a function of time and temperature was proposed. In this model, data from Hyne & Tyrer (1984), Hyne & Clark (1985) and Clark *et al* (1988) and equilibrium values shown in Table 1 were considered. Previous equations described in (3) to (5) were used to derive the kinetic parameters. Table 4 summarized these parameters for the CO_2 generation model.

The total quantity of generated CO_2 in the whole temperature interval was calculated from the following equation

$$N_{CO2} = \sum_i n_{Sand\_r}(i)_{initial} \cdot 1 - \exp(-K_i(T_i) \cdot t) \quad \text{.................... (8)}$$

Figure 3 shows the total CO_2 generated per kg of bitumen obtained after applying equation (8) and (5), and kinetics parameters from Table 4. The values of CO_2 generated at equilibrium time of 90 days (called "reference" in the figure) correspond to data from Table 1. Data from experimental results for two temperatures are also shown. In general, the generated CO_2 model reproduces well the equilibrium values at 90 days and follows the trend of experimental observations cited before.

Gas equilibrium in oil and aqueous phase

Equilibrium values of gases were included in the model based on experimental results and thermodynamic models reported in literature. Solubility of gases in water was calculated based on the thermodynamic model proposed by Duan & Sun (2003) and Duan *et al* (2007). This thermodynamic model is based on a specific particle interaction theory for the liquid phase and a highly accurate equation of state for the vapour phase. Parameters for the specific system were calculated after equalling the chemical potential of the solute in both phases and solving for the solubility of solute in the water phase and molar fraction of solute in the gas phase. The difference between model predictions and experimental data is within experimental uncertainty for a classical range of pressures and temperatures found during SAGD for both gaseous systems. We programmed the model for estimating the gas solubility in a MATLAB code using the fitted parameters reported by Duan & Sun (2003) and

Duan *et al* (2007) in their works. CO_2 solubility in oil phase was taken from PVT experiments on Athabasca bitumen done by the Alberta Research Council (ARC) and reported in a STARS template (stflu008.dat). No data about H_2S solubility in heavy oil was found in literature. This information was derived from H_2S partition coefficient (K-value) in gas-aqueous phase obtained from Duan model and H_2S K-value in aqueous-oleic phase according to the following expression

$$K^{go} = K^{gw} * K^{wo} \quad .... (9)$$

supposing that $K^{wo}_{H2S} \cong K^{wo}_{CO2}$.

Synthetic reservoir

A synthetic reservoir representing a generic formation in Athabasca oil sand (western Canada) was selected. The reservoir is 300 m deep with a pay-zone thickness of 40 m. Initial oil and water saturation in the pay zone are 0.8 and 0.2, respectively, and reservoir temperature is 10°C. The reservoir formation consist of clean sand, no heterogeneities were specified. The absolute permeability is 3000 mD in the horizontal direction and 1000 mD in the vertical direction. Porosity is fixed at 30%. Water-oil and gas-oil relative permeability curves are show in Figure 4 and 5. Oil viscosity as a function of temperature is shown in Figure 6. Detailed reservoir properties are listed in Table 5.

For the SAGD process, a horizontal production well with a length of 1000 m is placed 1.5 m above the bottom of the pay zone. A horizontal injection well with the same length is situated parallel to the producer with a vertical well spacing of 5 m. The horizontal spacing between well pairs is 100 m. Due to symmetry and the assumption of a homogeneous system, we model only half of the repeated unit. Our uniform 2D grid system contains 51 grid blocks in the y-direction and 40 grid blocks in the z-direction. The cells are 1 m wide and 1 m high.

A total number of thirteen components were included in the model. They consisted of water (formation or injected as steam), heavy oil (HO), CH_4, CO_2, H_2S, four reactive sulphur components ($HCS_r (1-4)$) and four reactive sand components ($Sand_r$ (1-4)). The initial mole fraction of fluid components and reactive components are listed in Table 6.

Furthermore, eight pseudo-chemical reactions are included in the reservoir model to describe the H_2S and CO_2 kinetic model. Activation energies were introduced as a function of temperature for each reaction specifying the reported value (Table 4) for temperature equal or higher than the corresponding temperature interval or a very high value of Ea for temperatures lower than the corresponding temperature.

CH_4 and H_2S were sourced in the bitumen while CO_2 was sourced in the water. H_2S and CO_2 were soluble in water and oil phase according to K-values tables described in the previous section. In this model, a linear mixing rule is applied to consider the viscosity reduction effects in the oil phase.

The thermal simulator, STARS, (2009 release) developed by CMG (Computer Modeling Group, Calgary) was used for the reservoir simulation runs.

Results

In the following sections gas emissions obtained for a SAGD process in bitumen are presented using the H_2S and CO_2

kinetics models. These kinetics models were previously validated, as shown next.

Kinetic model validation

Gas models were validated using two schemes to verify that experimental results were reproduced. First of all, kinetics models were programmed in MATLAB and compared to experimental results reported in literature. Figure 2 and 3 show H_2S and CO_2 model results and equilibrium values at 90 days from Table 1. Comparison of equilibrium results for gas emissions and those obtained by the kinetic model showed a relative error lower than 5.0 %.

The second validation scheme consists of building a reservoir model for each reactive system that reproduces the experimental conditions in a batch reactor. In this model, no injection, no production and no heat losses are permitted. In addition, the reservoir is kept at constant temperatures for comparing the amount of gas generated by oil mass present in the reservoir. A total of four runs for each reactive system were performed to analyze results at four temperatures (180, 200, 220 and 240°C). Although results are not shown in this article, no major deviations from equilibrium results were obtained.

Gas emissions at constant injection pressure

Three cases were run to study the effect of injection pressure on the gas emissions in a SAGD process. Saturated steam was injected at the corresponding injection pressure and steam quality was 0.8. After pre-heating the inter-well region to make the oil mobile, the steam was injected at a maximum pressure of 3500 kPa and the production well was operated at a fixed minimum bottom hole pressure of 1000 kPa. Two additional cases were run with steam injection pressures of 2500 and 1500 kPa. The simulation runs were terminated after 10 years of operation.

H_2S and CO_2 production results are shown in Figure 7 and Figure 8 as a function of injection pressure. Gas emissions are reported in gas mass per unit of produced oil volume. In particular for the H_2S generation, results are reported in units of t SO_2 per kbbl of produced oil to be in accordance with units normally used in field.

Gas emissions increase with steam injection pressure. When steam injection pressure increases, temperature of saturated steam injected in the reservoir also increases. According to the proposed gas models, gas formation is promoted by high temperatures, in particular, temperatures above 200°C (saturation pressure of 1555 kPa). Gas emissions show, in general, the typical three stages of SAGD production life, i.e., a steam chamber rising period (1 year), a plateau production stage (5 years), and a depleting stage due to the boundary effect. Figures 7 and 8 show that emissions reach a first production peak at the beginning of the exploitation period and rise to even higher values at the end of the steam injection period. This apparent increment in the gas generation is caused by the reduction in the oil production rate at the end of the injection period.

Figure 9 compares oil production rate and steam-to-oil ratio for different pressures for the described SAGD process. As expected, oil production rate increases when increasing injection pressure. However, the steam-to-oil ratio increases as a consequence of larger volumes of injected steam. Results also show that oil production rate decreases sharply at the end of the steam injection period for the high pressure cases (3500-2500 kPa). This reduction in oil production is the major cause of the increment of gas to oil ratio shown in Figure 7 and 8.

Gas emission results show that CO_2 model is more sensitive to increase in temperature than H_2S model: larger changes in CO_2 emissions are produced when steam injection pressure increase. This observation is confirmed from gas composition results shown in Figure 10 and 11. CO_2 molar fraction can vary from around 0.25 at 1500 kPa (saturated steam temperature ≈ 200°C) to 0.80 at 3500 kPa (243°C). On the other hand, H_2S molar fraction reduces with injection pressure due to relative large quantities of CO_2 produced.

Figure 12 shows values of SO_2 emissions as a function of injection pressure for some Canadian fields submitted to steam injection. Results obtained with our kinetics model (Figure 7) are in the same range as field observations, especially for the fields with lower SO_2 emissions (lower than 0.02 t SO_2 / kbbl bitumen). The discrepancy with the higher values (Firebag, Hangingstone…) may be explained by several factors: chemical composition of the bitumen and/or confinement of the steam chamber.

CO_2 emission values were not compared to field data. The majority of CO_2 emissions reported in literature for in situ CO_2 production under a SAGD process, are computed including CO_2 generation coming from the burning of gas for the purpose of generating steam.

Location of aquathermolysis reactions during SAGD

The location of the reactive zone is a question that arises when we study the gas formation during a SAGD process. Elementary considerations of chemical kinetics would suggest that the steam front and the fluid drainage region are the only regions of the SAGD steam chamber where reactions can occur. In these zones, high temperatures are reached and oil saturation is high enough to permit production of reaction products. In addition, condensate water in presence of carbonate rocks can cause carbonate decomposition to form CO_2. On the other hand, the region ahead of the steam front is too cold to permit reaction to proceed while the region behind the steam front has a residual content in bitumen which may not generate important gas quantities.

In order to verify where acid gases are formed, some profiles in the reservoir model were plotted at two stages. The first stage selected was after two years of steam injection and the second stage chosen was after 5 years of thermal recovery. Figure 13 shows temperature profiles, oil saturation profiles, sulphur molar fractions of reactive component $HCS_r(3)$, global mole fraction of H_2S and global mole fraction of CO_2. Plots show the inverse-triangle-shaped steam chamber growth. For the selected case, injection pressure is 2500 kPa which corresponds to a saturated steam temperature of 225°C, the maximum temperature reached in the steam chamber. Due to high temperatures, oil saturation is close to residual saturation in the center of the steam chamber. Small quantities of gases are generated in this region. On the contrary, the steam chamber boundary is the region where high temperatures and high concentrations of reactive components can be found. According to H_2S and CO_2 global mole fraction results, aquathermolysis reactions are produced in the most external zone of the steam chamber with a preferential reactive zone located in the uppermost part of the chamber.

This affirmation is supported by observations of H_2S and CO_2 phase distribution. Figure 14 and Figure 15 show the molar distribution of H_2S and CO_2 in three phases after two years of steam injection in the SAGD pair. In general, all acid gases are distributed in the uppermost external zone of the steam chamber.

Discussion

The proposed kinetic model based on experimental results for a particular Athabasca bitumen has proved to reproduce gas emissions reported in literature. This kinetic model that follows experimental observations and supposes a time decomposition function for the reactive components is able to generate gas plateaus at different temperatures. Reactions occur in parallel by grouping reaction sets for temperature intervals. A new reactive component is added to the reaction set for each temperature interval. In that way, kinetic permits reactive components to decompose progressively with temperature. As a result, acid gases are generated continuously in the whole temperature range (170-250°C) of steam injection during a SAGD process.

Figure 13 illustrates partially how the kinetic model works. When steam injection temperature is 225°C, just three reactive components are able to react and to produce acid gases according to equations (2) and (7). Consumption of reactant (1) to (3) progresses as a function of time; see for example reactive $HCS_r(3)$ in the figure. On the contrary, reactive components $HCS_r(4)$ and $Sand_r(4)$ do not react because steam temperature is not high enough for activating the last reactive set (T > 230°C).

The proposed kinetic model has some weaknesses. This model does not consider the effect of condensate steam in the acid gas formation. Experimental evidences show that steam condensate play a major role in the acid gas formation but the way how condensate water interacts with reactives is not clearly understood. Secondly, the CO_2 model does not consider the chemical interactions that imply carbon dioxide dissolution in water. In third place, the application of this model is limited to the idealized Athabasca bitumen analyzed in this paper. In addition, the reaction scheme is considerably simpler than reality, which may explain why we had to suppress reactions below some critical temperatures.

However, the followed methodology may be applied to any oil sand that has gas emission data for different temperatures and times. The aquathermolysis mechanism is not limited to the SAGD process, and our approach is also expected to be used for modeling acid gas production in other thermal processes (Huff 'n Puff, steam-drive). The simple model proposed in this work is a pragmatic approach to integrate acid gas generation models and gas partitioning in a reservoir model. In addition, our model allows taking into account reaction kinetics, which is something that models like those presented by Gillis & Thimm (2000) do not do.

The presence of CO_2 in the oil phase has been identified as a source of viscosity reduction in literature (Thimm, 2000). According to Figure 15, CO_2 molar concentration in the oil phase can reach 17% in the upper zone of the steam chamber boundary. A priori a viscosity reduction may be expected in the oil phase, but we believe that viscosity reduction may be weak at least at high temperature (T≈ 225°C), where oil viscosity is low.

Conclusions

- A novel kinetics model to mimic H_2S and CO_2 generation under aquathermolysis conditions has been tested and integrated in a reservoir simulation. The model is able to reproduce gas plateaus at different temperatures. In addition, the model includes partitioning of H_2S and CO_2 in oil/gas/water phase.
- Comparison of H_2S production results obtained by the reservoir model with field results shows that predicted gas emissions are of the same order of magnitude as those reported at field scale.

Acknowledgement

NOMENCLATURE

N	=	total number of mole of components
n	=	number of mole per temperature interval
K	=	rate constant, day^{-1}
t	=	time, days
A	=	pre-exponential factor, day^{-1}
Ea	=	activation energy, J/gmol
K^{go}	=	gas-oil phase equilibrium ratio
K^{gw}	=	gas-water phase equilibrium ratio
K^{wo}	=	water-oil phase equilibrium ratio

Sub-indices

i	=	temperature interval number
p	=	reactive number in temperature interval
$initial$	=	initial values at t=0
$reactive$	=	reactive component

REFERENCES

1. ABERCOMBIE, H.J., and HUTCHEON, I.E., "Remote monitoring of water-rock-bitumen interactions during steam assisted heavy oil recovery", 5th Int. Symp. on Water-Rock Interaction Extend. Abstr., pp. 1-4, 1986.
2. BIRD G.W., GUNTER, W.D. and KIRK, J.S., "Mineralogical reactions during in situ steamflooding of the Clearwater Formation: Implications for recovery", Can. Soc. Pet. Geol 1986 Convent., Prog. Abstr., p.27 (abstract).
3. BURGER J., SOURIEAU P., COMBARNOUS M., 1985, *"Thermal methods of oil recovery"*, Ed. Technip, Paris, France, 430 pp.
4. CATHLES L.M., SCHOELL, M., SIMON, R."CO_2 generation during steamflooding: a geologically based kinetic theory that includes carbon isotope effects and applications to high temperature steamfloods". Int. Symp. on Oilfield Chemistry, San Antonio, Texas, SPE paper N° 16267, 1990.
5. CATHLES L.M., SCHOELL, M., SIMON, R. "A kinetic model of CO_2 generation and mineral and isotopic alteration during steamflooding", SPE Reservoir Engineering, November 1990, pp. 524-530.
6. CLARK R.A., DOWLING, N.I. and HYNE, J.B., "Oil sand - hot water/steam chemical reactions", Alberta Sulphur Research LTD, Quarterly Bulletin, Vol. XXII, N° 1, April - June 1985.
7. CLARK, P., and HYNE, J., "Steam-Oil Chemical Reactions: Mechanism for the Aquathermolysis of Heavy Oil"; AOSTRA Journal of Research, Vol. 1, No. 1, pp. 15-20, 1984.
8. CLARK, P.D., CLARKE, R.A., LESAGE, K. L. and HYNE, J.B., "The behaviour of various oil sands towards high temperature steams", AOSTRA Paper No. 54, Fourth UNITAR/UNDP International Conference on heavy crude and tar sands, Proceedings: August 7-12, 1988, Edmonton, Alberta, Canada.
9. DUAN Z. and SUN R. "An improved model calculating CO_2 solubility in pure water and aqueous NaCl solutions from 270 to 533K and from 0 to 2000 bar", Chemical Geology, Vol. 193, 2003, pp. 257-271.
10. DUAN Z., SUN R., LIU R. and ZHU C., "Accurate thermodynamic model for the calculation of H_2S solubility in pure water and brines", Energy and Fuels, Vol. 21, 2007, pp. 2056-2065.
11. GILLIS, K.A., THIMM, H.F., "Simulation of gas production in SAGD", SPE/Petroleum Society of CIM 65500, Paper presented at SPE/PS-CIM International Conference on Horizontal Well Technology held in Calgary, Alberta, Canada, 6-8 November 2000.
12. GUNTER W.D., BIRD, G.W., *"CO_2 production in tar sand reservoirs under in situ steam temperatures: reactive calcite dissolution"*, Chemical Geology, Vol. *70,* 1988, pp. 301-311.
13. HYNE J., *"A synopsis of work on the chemical reaction between water (steam) and heavy oil sands during simulated steam stimulation"*, Synopsis report N°50, AOSTRA Publication Series, 1986.
14. HYNE J., *"Aquathermolysis of heavy oils"*, 2nd Conference on heavy crude oils and tar sands, UNITAR, Caracas, Venezuela, February 7-17, 1982, pp.23.
15. HYNE J.B. and TYRER J.D., "Use of hydrogen-free carbon monoxide with steam in recovery of heavy oil at low temperature", Patent number US 4487264, 1984.
16. HYNE J.B., CLARK, P. D., "Additive for inclusion in a heavy oil reservoir undergoing steam injection", Patent number US 4506733, 1985.
17. *LAMOUREUX, V., LORANT, F., "Experimental evaluation of H2S yields in reservoir rock submitted to steam injection", Paper number D08, Paper presented at 13th European Symposium on Improved Oil Recovery — Budapest, Hungary, 25 - 27 April 2005b.*
18. *LAMOUREUX, V., LORANT, F., "H2S artificial formation as a result of steam injection for EOR: a compositional kinetic approach", SPE/PS-CIM/CHOA SPE-97810, PS2005-375, Paper presented at the 2005 SPE International Thermal Operations and Heavy Oil Symposium held in Calgary, Alberta, Canada, 1–3 November 2005a.*
19. SALAZAR A., EMBID, S., RUSINEK, L., "Simulation of H2S production of H2S during steam injection", 3rd EOR International Symposium, Proceedings Vol 2, 1989, pp. 1101, 1103-1127.
20. THIMM, H.F., *"A general theory of gas production in SAGD operations"*, CIPC, Calgary, Canada, June 4-8, 2000. Paper number 2000-17.
21. THIMM, H.F., *"Prediction of hydrogen sulphide production in SAGD projects"*, JCPT, Volume 47, N° 1, 2008.

Table 1. Equilibrium gas production from Athabasca oil sand submitted to aquathermolysis after 90 days of reaction time.

Temp. (°C)	(mls gas STP/kg oil sand)	
	H_2S	CO_2
180	0	23
200	23	875
220	45	5020
240	68	8570

Table 2. Physical characterization of an Athabasca bitumen and fractions.

	Whole bitumen	Resins	Asphaltenes
Fraction wt%	-	32.5	14.6
Avg. molecular w.	500	762	7464
C (wt. %)	-	80.3	77.6
H (wt. %)	-	9.7	7.8
N (wt. %)	-	0.7	1.2
O (wt. %)	-	3.4	2.0
S (wt. %)	5.0	5.9	8.3
H/C atomic ratio	-	1.45	1.2
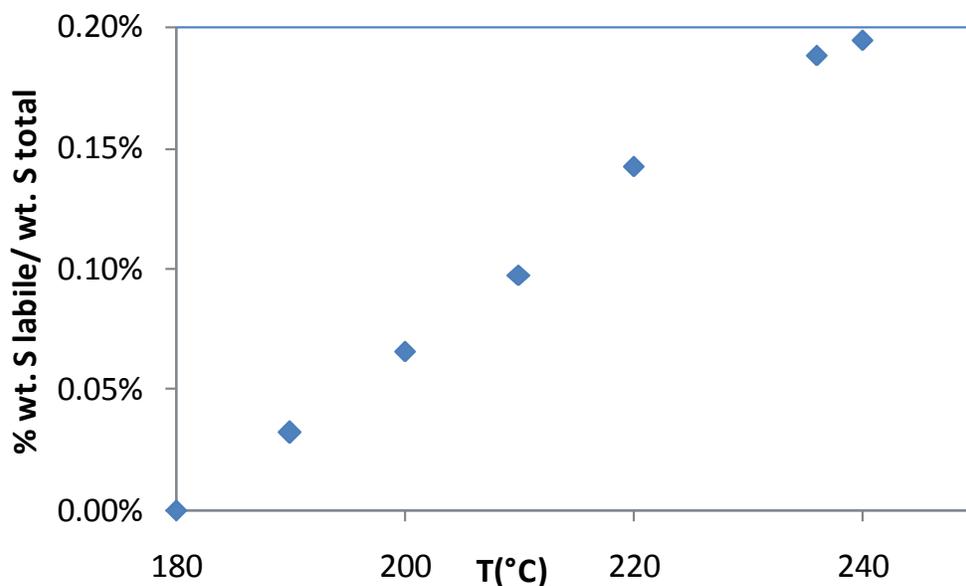
Figure 1. Percentage of labile sulphur per total sulphur in oil sand as a function of temperature at equilibrium time.

Table 3. Initial molar mass of reactive components for the H_2S and CO_2 kinetic model.

	HCS_r	Sand_r
	(gmol HCS_r/gmol bitumen)	(gmol Sand_r/m3 PV)
Reactant (1)	1.035E-08	1.0
Reactant (2)	2.381E-04	30.8
Reactant (3)	2.346E-04	150.5
Reactant (4)	2.264E-05	128.8
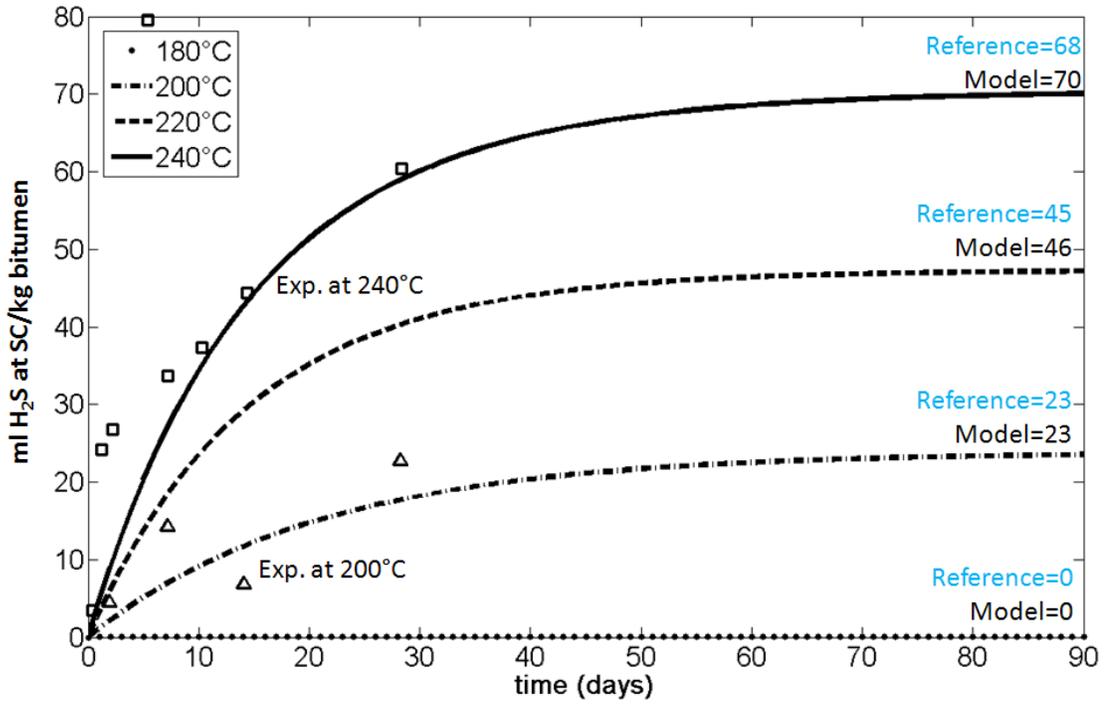
Figure 2. Comparison of H_2S formation model and experimental values and equilibrium values (reference) from Table 1.
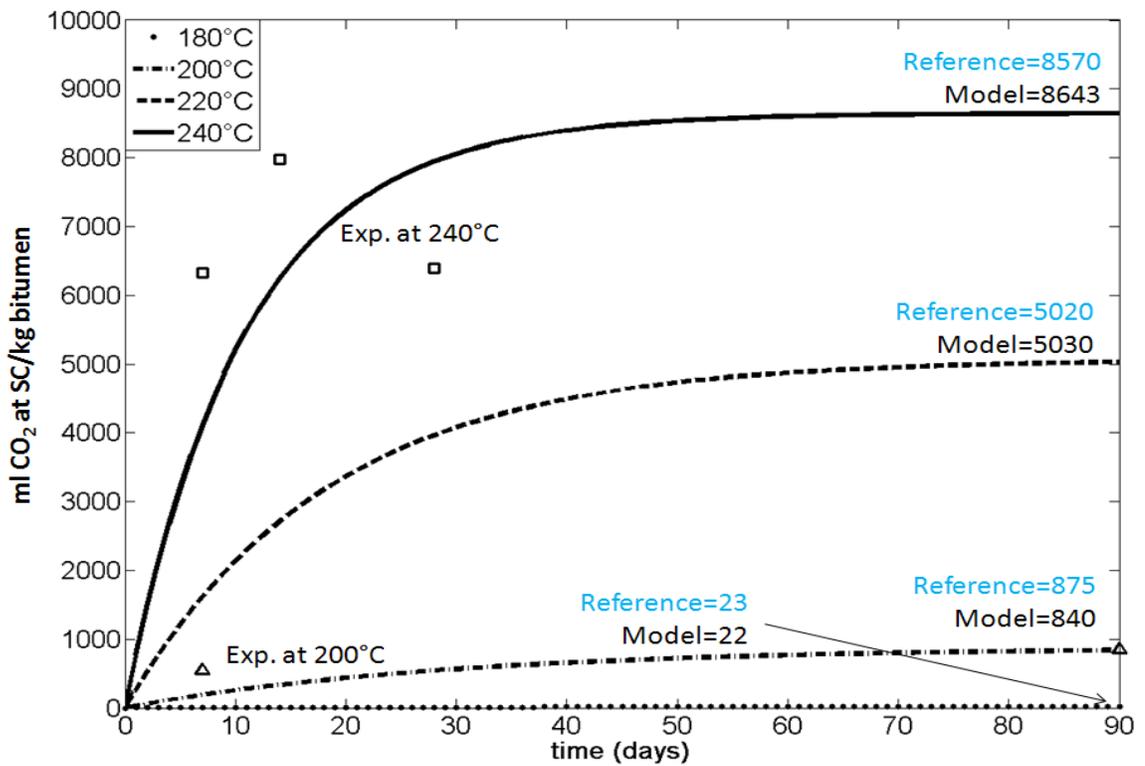
Figure 3. Comparison of CO_2 formation model and experimental values and equilibrium values (reference) from Table 1.

Table 4. Parameters for the H_2S and CO_2 kinetic model.

	Temperature interval	H_2S model		CO_2 model	
		A(1/day)	Ea(J/gmol)	A(1/day)	Ea(J/gmol)
K1	170-190°C	4142	44035	4.3481E05	64098
K2	190-210°C	12581	49066	3.4008E05	63364
K3	210-230°C	86799	58271	1.3888E06	70079
K4	230-250°C	86799	59761	1.3888E06	71370
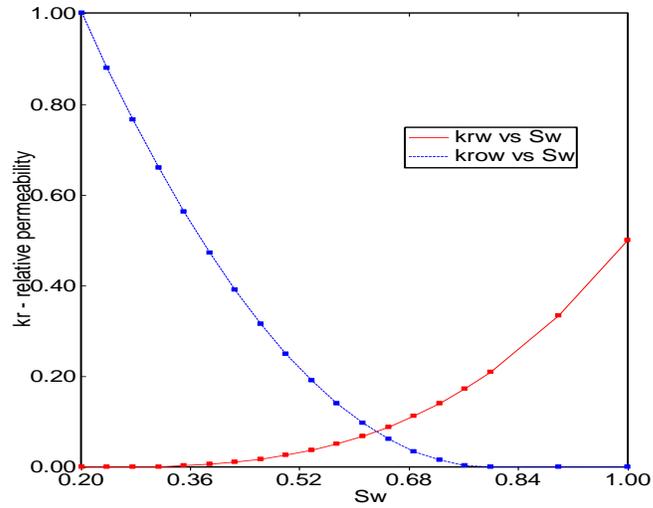
Figure 4. Water-oil relative permeability used in the reservoir model.
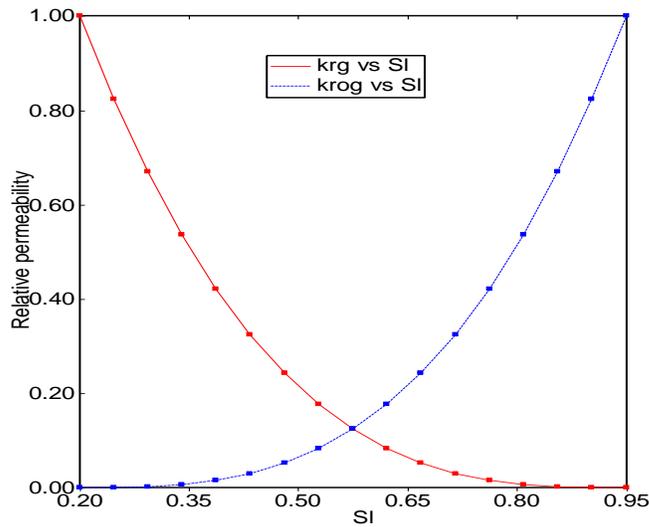
Figure 5. Gas-oil relative permeability used in the reservoir model
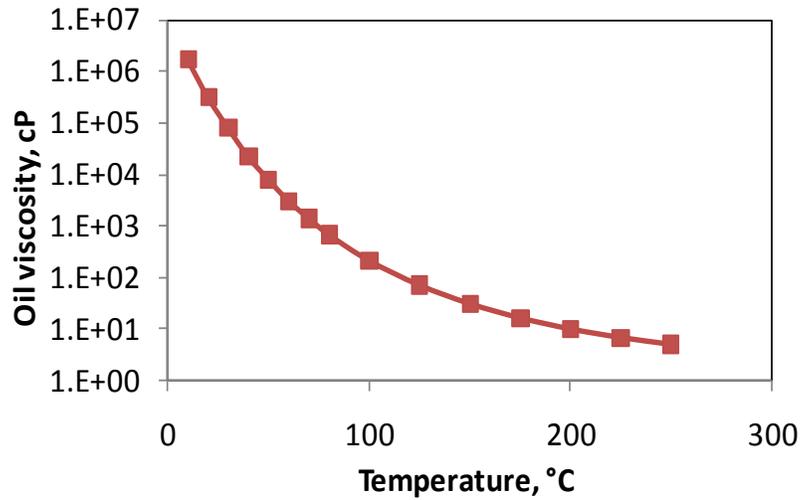
Figure 6. Oil viscosity vs. temperature used in the reservoir model.

Table 5. Reservoir properties.

Properties	
Reservoir depth	300 m
Reservoir thickness	40 m
Porosity	0.30
Horizontal permeability	3000 mD
Vertical permeability	1000 mD
Oil viscosity at RC	1.7 E+06 cP
Initial pressure at reservoir top	1000 kPa
Initial temperature	10°C
Initial oil saturation	0.8
Initial water saturation	0.2
Oil gravity	8 API

Table 6. Initial values of fluids and reactive components in the reservoir simulation model.

Components	
Heavy oil (HO)	0.9623 mol HO/mol bitumen
CH4	0.037 mol CH4/mol bitumen
HCS_r(1)	1.0353E-08 mol HCS_r/mol bitumen
HCS_r(2)	2.3812E-04 mol HCS_r/mol bitumen
HCS_r(3)	2.3460E-04 mol HCS_r/mol bitumen
HCS_r(4)	2.2640E-04 mol HCS_r/mol bitumen
Sand_r(1)	1.00 mol Sand-r/m^3 PV
Sand_r(2)	30.78 mol Sand-r/m^3 PV
Sand_r(3)	150.47 mol Sand-r/m^3 PV
Sand_r(4)	128.79 mol Sand-r/m^3 PV
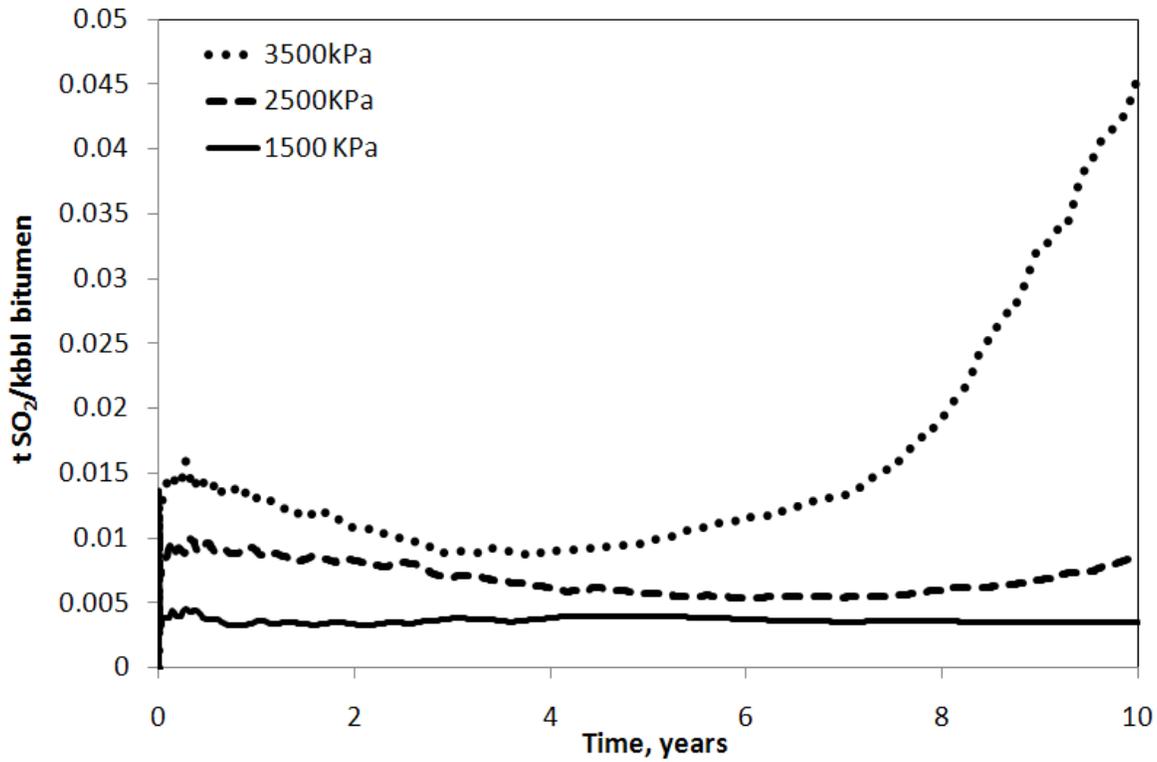
Figure 7. SO$_2$ emissions per produced oil volume for different injection pressures.
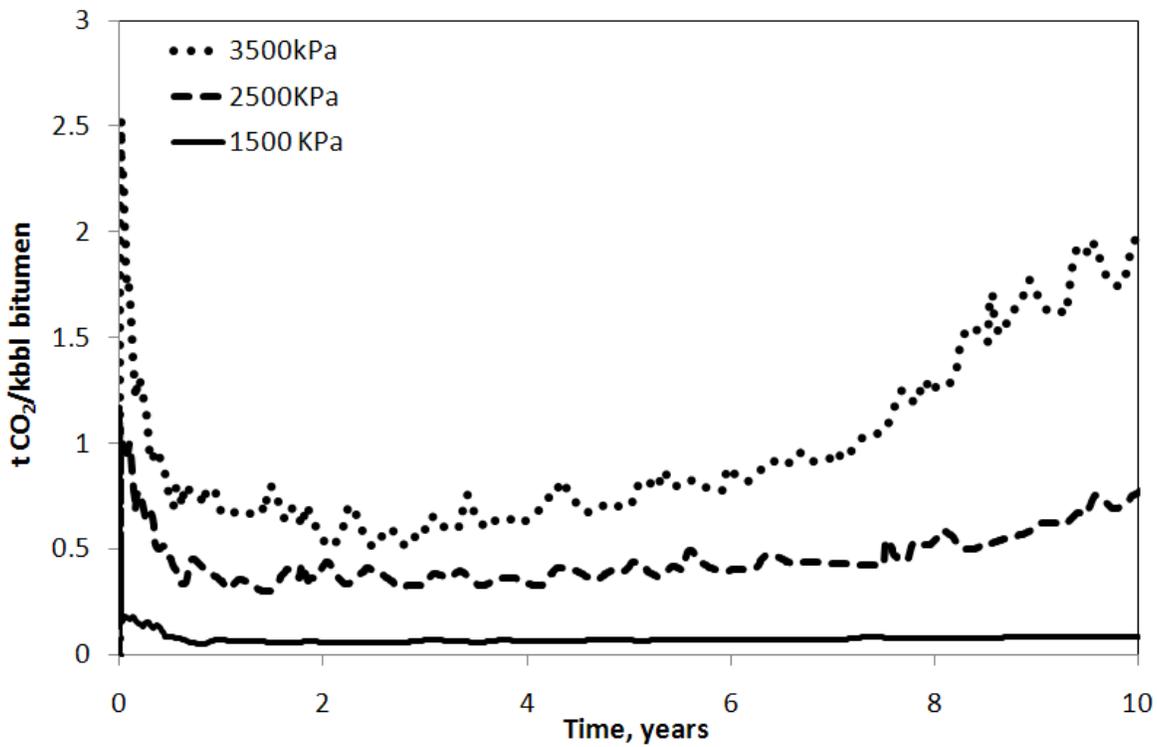

Figure 8. CO$_2$ emissions per produced oil volume for different injection pressures.
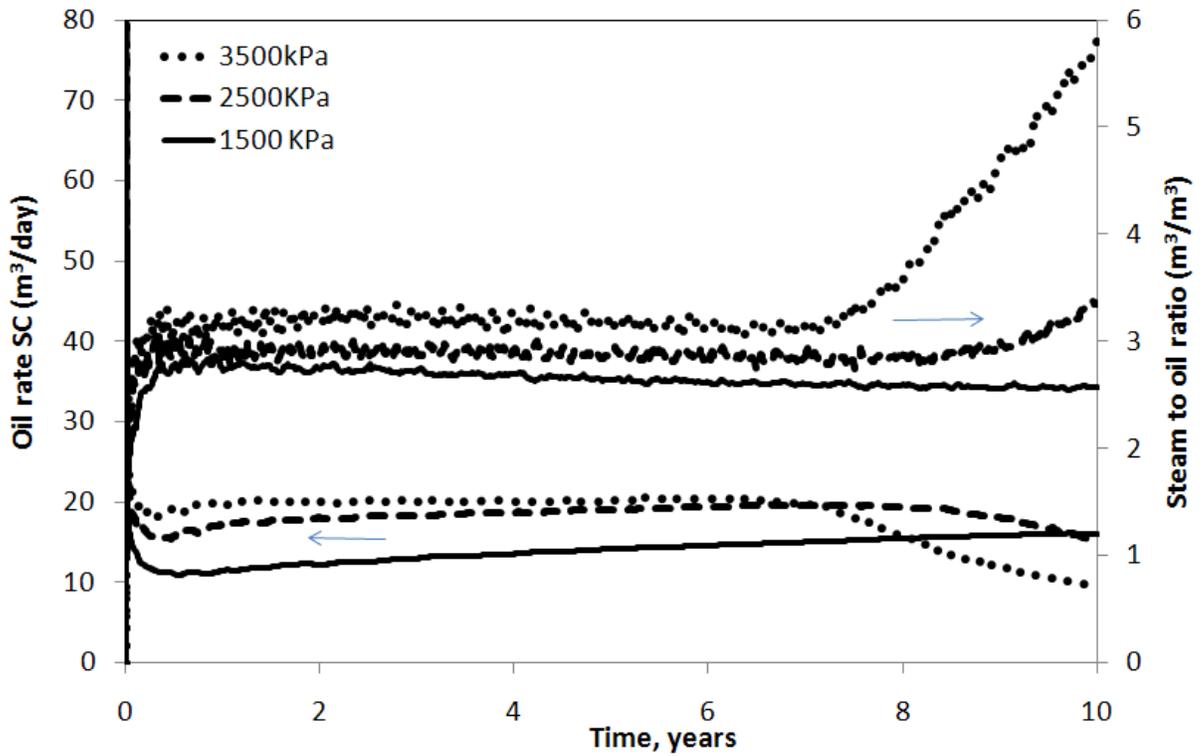
12

Figure 9. Oil rate and steam-oil ratio (instantaneous) for different injection pressures.
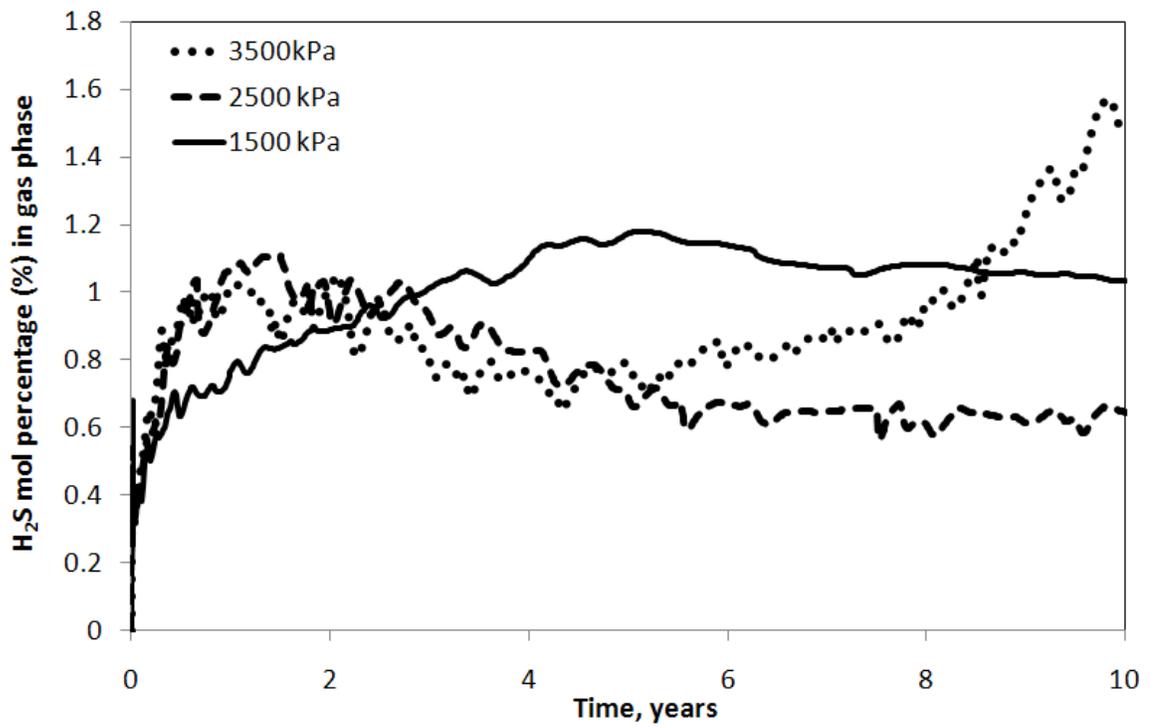

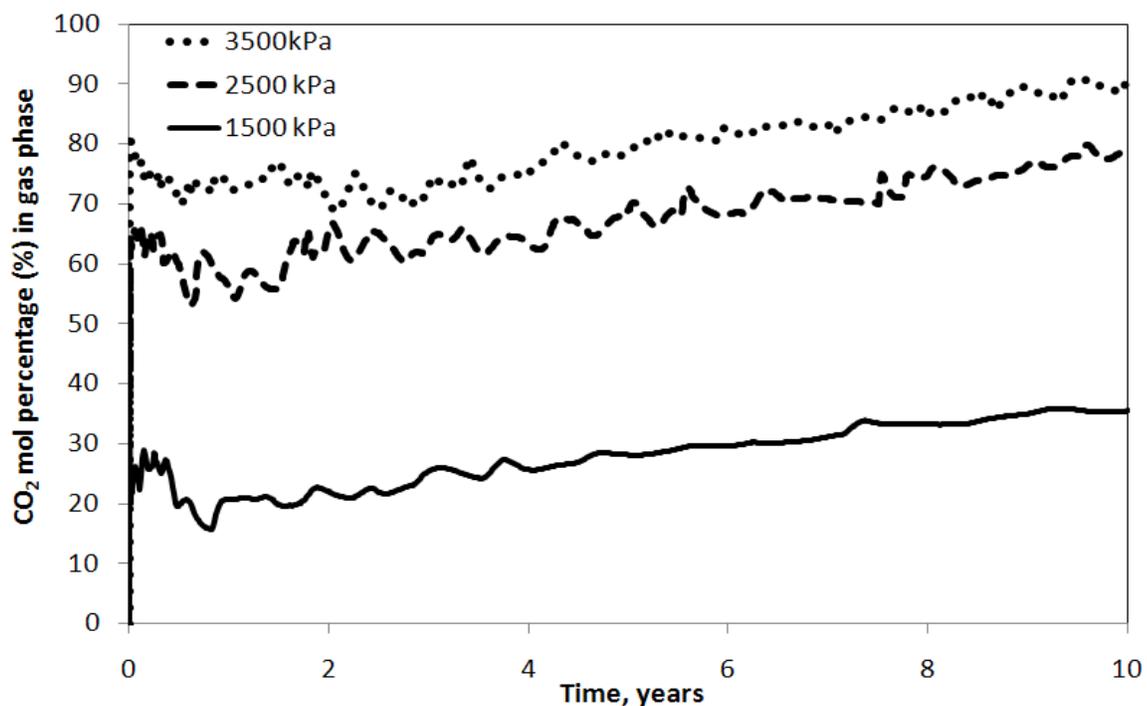Figure 10. H₂S gas composition for different injection pressures.

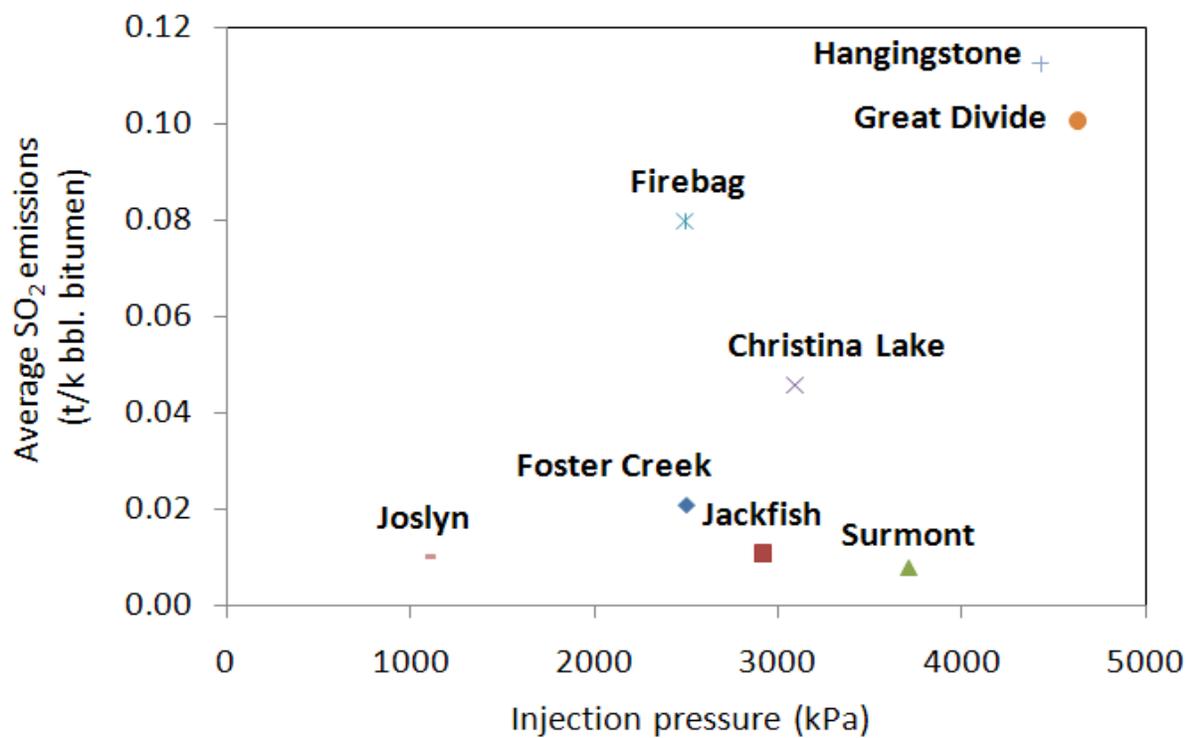Figure 11. CO_2 gas composition for different injection pressures.

Figure 12. Average SO_2 emissions vs. operation pressure in some Canadian steam injection projects.
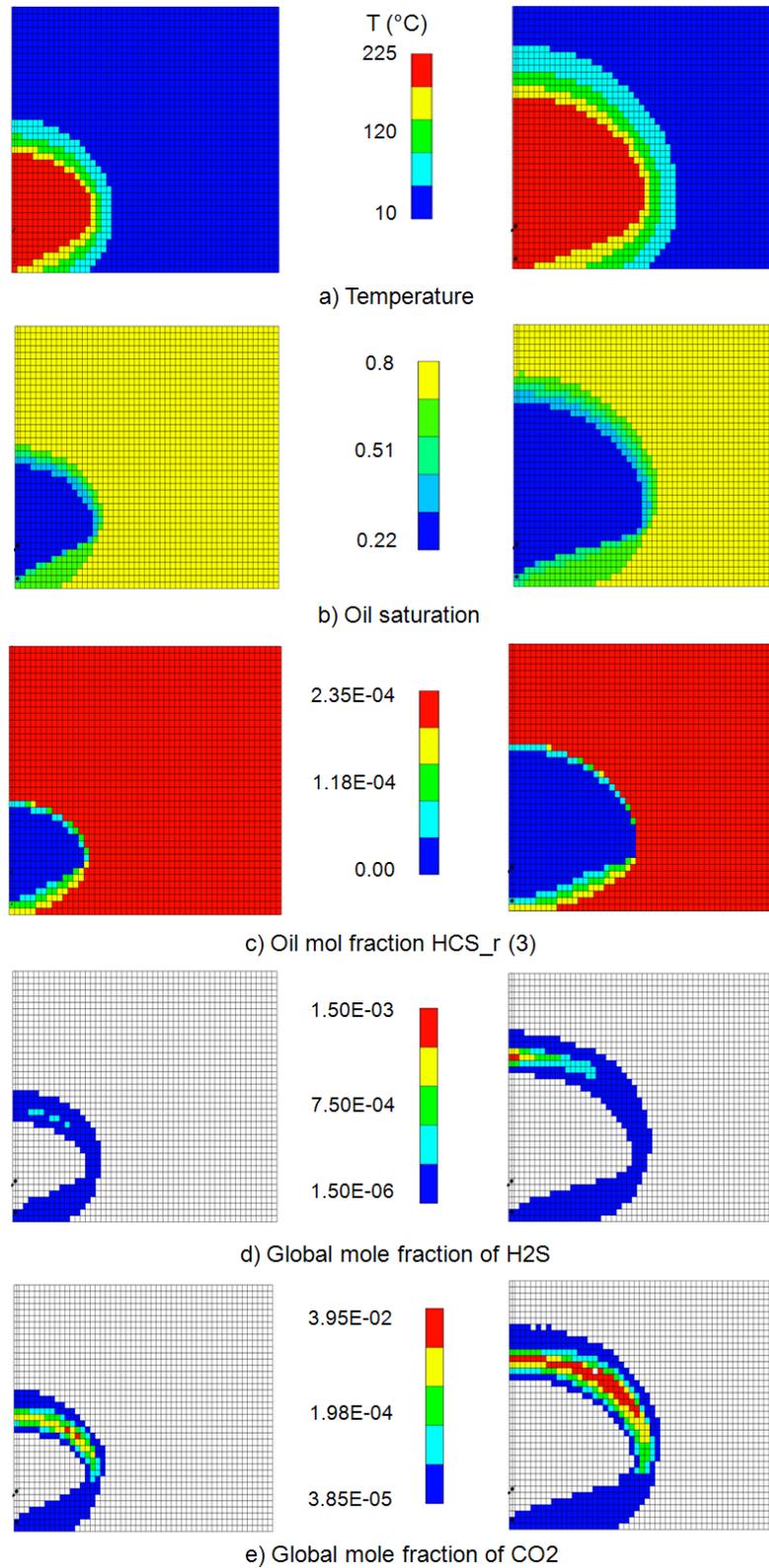
Figure 13. Profiles for SAGD after 2 years (left column) and after 5 years (right column) of steam injection. Injection pressure= 2500 kPa. (a) Temperature, (b) Oil saturation, (c) Oil mol fraction of HCS-r(3), (d) Global mole fraction of H_2S, and (e) Global mole fraction of CO_2

a) H$_2$S mole fraction in gas phase   b) H$_2$S mole fraction in oil phase   c) H$_2$S mole fraction in aqueous phase
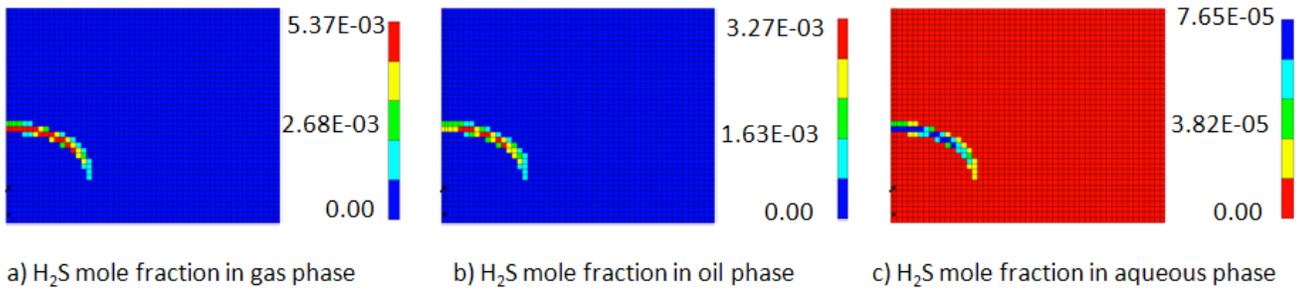
Figure 14. Molar distribution of H$_2$S in three phases after 2 years of steam injection. Injection pressure= 2500 kPa. (a) gas phase, (b) oil phase, (c) water phase.

a) CO$_2$ mole fraction in gas phase   b) CO$_2$ mole fraction in oil phase   c) CO$_2$ mole fraction in aqueous phase
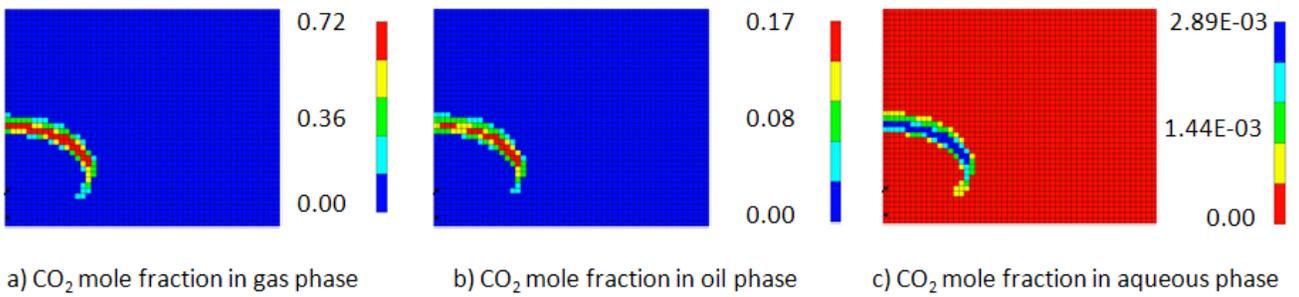
Figure 15. Molar distribution of CO$_2$ in three phases after 2 years of steam injection. Injection pressure= 2500 kPa. (a) gas phase, (b) oil phase, (c) water phase.